ISSN (Print) 1226-1750
ISSN (Online) 2233-6656
Journal of Magnetics 27(3), 242-249 (2022) https://doi.org/10.4283/JMAG.2022.27.3.242

Quasi-linear and Plateaus-like Tunneling Magnetoresistance in Graphene-based Tunable Magnetic Barrier Nanostructures

Chaiyawan Saipaopan[1] and Wachiraporn Choopan[2]*

[1]*Demonstration School, Bansomdejchaopraya Rajabhat University, Itsaraphap Road, Hiran Ruchi, Thonburi, Bangkok 10600, Thailand*
[2]*Department of Biomedical Engineering, College of Health Science, Christian University of Thailand, Donyaihom District Nakhonpathom 73000, Thailand*

(Received 12 July 2022, Received in final form 19 September 2022, Accepted 22 September 2022)

The effect of electrostatic and magnetic vector potentials pattern on electrical properties and the tunneling magnetoresistance in graphene junction with periodic magnetic vector potentials are theoretically investigated using the transfer matrix method. The magnetic structure on graphene can control the direction of the magnetizations which correspond to the parallel and anti-parallel (AP) configurations. In AP magnetic structures with the applied gate voltage pattern, U_A ($U_1 = U_2$), the shift of the conductance-peak position as a function of Fermi energy. The peak corresponds to resonant tunneling, where the incidence energy of the tunneling electron equals the confinement energy, and the conductance peak decrease approximately linearly with increasing electrostatic potential. The peak position occurs at $E_F = 0.5U$ where it is shifted to higher Fermi energy with higher gate potential, but for the case of U_B ($U_1 = -U_2$), the peak height is reduced rapidly, and the width increase as gate potential increases. Because of the periodic magnetic field with zero spatial average in the antiparallel structure, we found that the minimum conductivity decreases with increasing magnetic energy. They show suppression of Klein tunneling which occurs in the zero-conductance plateaus and leads to the robust magnetoresistance plateau and large positive magnetoresistance appears below magnetic energy. For the case of U_A and E_F more than magnetic energy, we found that the quasi-linear magnetoresistance feature is applied by an electric field instead of the usual magnetically driven magnetoresistance.

Keywords : magnetic vector potential, tunneling magnetoresistance, quantum transport, graphene

1. Introduction

Graphene is a two-dimensional honeycomb lattice of carbon atoms which was quickly shown [1-3] that the low-energy quasiparticle in graphene mimic the behaviors of massless relativistic Dirac fermion. Graphene is a gapless semiconductor in which conduction and valence band edges meet at K and K' in the Brillouin zone. The quasiparticles in graphene have long spin-flip scattering and spin lifetime at room temperature [4]. The type of the charge carriers (either electrons or holes) could be selected by using electric doping on the graphene [5, 6] and the carrier density can be manipulated by applying the electric field effect. By depositing EuO film [7], it can be induced the exchange splitting on graphene as ferromagnetic graphene (FG) when the carriers pass through this layer to split into two subbands of spin [8]. While the theoretical investigation reported that the magnetic insulator EuO can induce a large proximity effect on graphene and exhibit a large exchange-splitting band gap of about 36 meV. [9, 10]. For controlling the direction of the exchange field, which is perpendicular to the graphene plane there are several studied in Refs. 9, 11-15.

One of the main obstacles to the development of the device is scarce the spin-polarized current source. However, Rashba [16] has theoretically studied and suggested that the use of tunnel contact can solve the problem of the mismatch between the ferromagnetic metal and the normal conductor junction. At the same time, the solving problem of the mismatch of the ferromagnetic metal into a semiconductor can introduce spin-dependent interface resistance, and spin injection [17, 18]. The material that is called half-metallic has been predicted that electrical current can be completely spin-polarized. While Son et al. [19] predicted that the half-metallic in two-dimensional

*Corresponding author: Tel: +66-81-163-7176
Fax: +66-34-274-500, e-mail: touch2wachi@gmail.com

graphene nanoribbon can be induced by external electric fields, which new open up graphene-based spintronic devices.

Besides, the Rashaba spin-orbit interaction plays a crucial role in the control spin because of its strength that can be controlled by the gate potential. Recently, the contacting graphene with ferromagnetic insulator EuO deposited on top of the graphene sheet can induce the proximity exchange [7]. It is found that the exchange field (H) is about 5 meV in an adjacent ferromagnetic insulator. At the same time, the strength of the exchange field can be enhanced by applying an external electric field perpendicular to the graphene sheet [20]. T. Yokoyama [21] proposed that the spin current shows an oscillatory behavior in the ferromagnetic-gate graphene structure. While the effect of the exchange field on the shifting spin conductance in the opposite direction, it is found that the phase shift can be estimated to be $2H$ [22]. The main aim of graphene-based spintronics is a perfect spin-polarized source, Zhai and Chang [23] have investigated the spin-dependent theoretically in the graphene monolayer. They found that the magnetic-electric barrier can block the transmission for antiparallel, but only can not produce a high spin polarization. However, Liewian *et al.* [24] suggested that the perfect spin-polarized (≈ 100 %) can be achieved by combining the orbital effect and the Zeeman interaction in graphene junction. Besides, Song *et al.* [25-27] demonstrated that a 100 % spin polarization, more like a half-metallic can be achieved by using a single magnetic vector potential barrier structure.

In this paper, we investigate the wave-vector-dependent transport of massless Dirac electrons through graphene with nanostructured magnetic barriers. It can be realized by periodic ferromagnetic nanostrips placed on top of the graphene layer where this magnetic system creates the magnetic vector potential (MVP) barrier on the graphene. For the presence of the orbital effect in MVP barriers, we study the difference between the transmission and conductance of the parallel and antiparallel magnetization configurations. By manipulating the two magnetization configurations, we propose the non-trivial magnetoresistance base on the wavevector-dependent tunneling which is the result of the orbital effect of inhomogeneous magnetic fields.

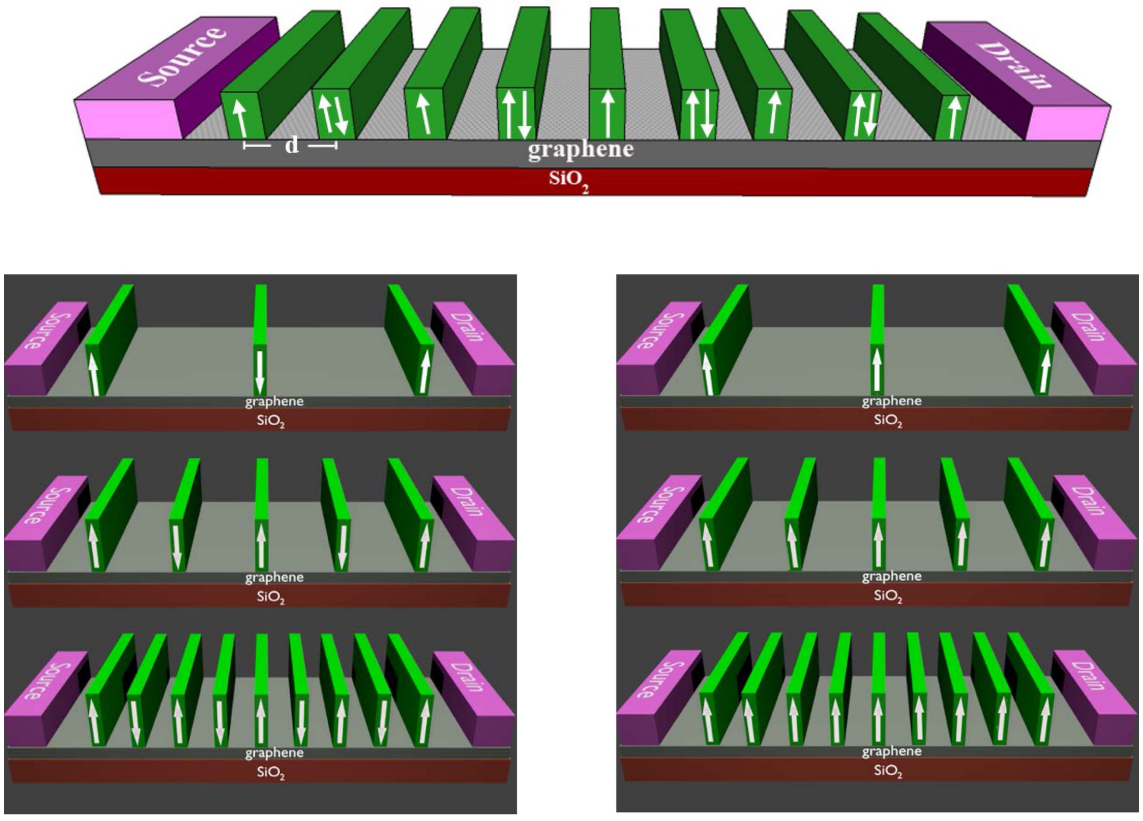

Fig. 1. (Color online) Schematic diagram of the graphene system with tunable magnetic barriers. (a) The antiparallel and (b) parallel delta-function-shaped magnetic structures.

2. Theoretical Model

The study of magnetoresistance from a change in the magnetization structure perpendicular to the graphene plane. The analysis of such a problem can be achieved by considering the electrons in graphene as Dirac particles that propagate through a multiple magnetic vector potential barrier, where a set of magnetic systems can be manipulated by a parallel or antiparallel configuration as shown In Fig. 1(a) and 1(b). In this model, it is possible to create nanoscale magnetic strips using EuO or yttrium iron garnet (YIG) magnetic materials. That can generate the orbital energy in a field of 1 T, the comparable spin splitting order of 25 meV [28]. While the width of the magnetic stripe can be reduced to very small to 10 nm using nanolithography [29, 30]. This model can be considered as a magnetic vector potential superlattice structure, which characterizes the parallel and antiparallel vector potential profiles, which is explained by the A_y equation. The magnetic field is placed in the z-axis direction, which is perpendicular to the graphene plane (x, y). In this paper, the magnetic barrier can be approximated as a set of Dirac-δ function. The magnetic profile can be written as a function of $\vec{B} = B_z(x)\vec{z}$

$$B_z(x) = \sum_{n=0}^{m} Bl_B\delta(x+2nd) \mp \sum_{n=0}^{m-1} 2Bl_B\delta(x+(2n+1)d) \quad (1)$$

where m is the number of periods of the magnetic vector potential and the minus or plus sign for a parallel or antiparallel magnetic structure, respectively. The term $l_B = \sqrt{\frac{\hbar}{eB}}$ is magnetic length. For an antiparallel magnetic structure, the magnetic fields can be described as the magnetic vector potential in the Landau gauge.

$$A_y^{AP}(x) = \sum_{n=1}^{m} \begin{Bmatrix} Bl_B\Theta(x-(n-1)d)\Theta(nd-x) \\ -Bl_B\Theta(x-nd)\Theta(2nd-x) \end{Bmatrix} \quad (2)$$

and an example of a magnetic vector potential function for a parallel structure at m = 1.

$$A_y^{P}(x) = Bl_B \begin{Bmatrix} \Theta(x-d)\Theta(d-x) + 3\Theta(x-d)\Theta(2d-x) \\ +4\Theta(x-2d) \end{Bmatrix} \quad (3)$$

where d is the distance between the magnetic stripe, and B is the magnetic field, which is the Heaviside step function. The real value of B = 0.1 T, gives the value of the magnetic length of 81.1 nm and E_0 = 7 meV, which are magnetic energy, and can be calculated from $E_0 = \frac{\hbar v_F}{l_B}$.

Therefore, the electron model in this proposed graphene can be described by the following massless Dirac Hamiltonian,

$$H_{AP,P} = \hbar v_F[\sigma_x.k_x + \sigma_y.(k_y - \frac{eA_y^{AP,P}(x)}{\hbar})] \quad (4)$$

where $v_F \approx 0.86 \times 10^6$ m/s is the Fermi velocity of the particles in graphene, σ_x and σ_y are the Pauli spin matrices, k_x and k_y are wave vectors of electrons in the xy plane on graphene.

In this work, we apply the transfer matrix method to calculate transmission probability. Thus, we assign that the solution of the Hamiltonian (eq. 4) as $\Psi = (\psi_A, \psi_B)$, ψ_A and ψ_B is continuous. In addition, due to the symmetry of the solution in the y direction, $\Psi = (\psi_A, \psi_B)$ can be rewritten as $\Psi = (\psi_A, \psi_B)e^{ik_y}$. To investigate the scattering problem at the junction for each magnetic vector potential barrier, the solution is

$$\begin{pmatrix} \Phi_A(x_j) \\ \Phi_B(x_j) \end{pmatrix} = R_j(E,k_y)\begin{pmatrix} \Phi_A(x_j) \\ \Phi_B(x_j) \end{pmatrix} \quad (5)$$

Where $R_j(E,k) = \begin{pmatrix} 1 & 0 \\ i\sin\theta_j & \cos\theta_j \end{pmatrix}$, $\theta_j = \arcsin(\frac{k_y - \frac{e}{c}A_j}{k_j})$.

Hence, the solution of the particle travel across the series of vector potential barriers is

$$\begin{pmatrix} \Phi_A(x_{j-1}+\Delta x) \\ \Phi_B(x_{j-1}+\Delta x) \end{pmatrix} = T_j(\Delta x, E, k_y)\begin{pmatrix} \Phi_A(x_{j-1}) \\ \Phi_B(x_{j-1}) \end{pmatrix}, \quad (6)$$

where

$$T_j(\Delta x, E, k_y) = \begin{pmatrix} \cos(q_j\Delta x) & i\sin(q_j\Delta x) \\ i\sin(q_j\Delta x+\theta_j) & \cos(q_j\Delta x+\theta_j) \end{pmatrix}.$$

and

$$q_j = sign(k_j)\sqrt{k_j^2 - (k_y - \frac{e}{c}A_j)^2}$$

Here, j indicates the number of the vector potential and T_j is the transfer matrix in the j^{th} potential barriers. Therefore, eq. (5) can be reformed to

$$\begin{pmatrix} \Phi_A(x_{j-1}+\Delta x) \\ \Phi_B(x_{j-1}+\Delta x) \end{pmatrix} = M_j(\Delta x, E, k_y)\begin{pmatrix} \Phi_A(x_{j-1}) \\ \Phi_B(x_{j-1}) \end{pmatrix}, \quad (7)$$

where

$$M_j(\Delta x, E, k_y) = T_j(\Delta x, E, k_y) R^{-1}(E, k_y)$$
$$= \begin{pmatrix} \frac{\cos(q_j \Delta x)}{\cos\theta_j} & \frac{i\sin(q_j \Delta x)}{\cos\theta_j} \\ \frac{i\sin(q_j \Delta x + \theta_j)}{\cos\theta_j} & \frac{\cos(q_j \Delta x + \theta_j)}{\cos\theta_j} \end{pmatrix}. \quad (8)$$

We notice that eq. (8) satisfies $\det M_j = 1$, which correspond to the solution of multiple barriers in the transfer matrix method,

$$\Phi_{out} = X \Phi_{in}$$

where Φ_{out}, Φ_{in} and X stands for the outward solution, inward solution, and transfer matrix respectively. For the sake of simplicity, we rewrite the product of M_j to X with the matrix element x_{ij} as

$$\mathrm{X} = \prod_{j=1}^{N} M_j(\Delta x, E, k_y) = \begin{pmatrix} x_{11} & x_{12} \\ x_{21} & x_{22} \end{pmatrix}. \quad (9)$$

To comprehend the above formula, we introduce the X matrix through the parallel structure with a period of MVP:

$$\mathrm{X} = M_1 M_2 M_3 = T_1(\Delta x) R_1^{-1} T_2(2\Delta x) R_2^{-1} T_3(3\Delta x) R_3^{-1} \quad (10)$$

where $q_{1,2,3} = \sqrt{k^2 - (k_y - \frac{e}{c} A_{1,2,3})^2}$ and

$$\theta_{1,2,3} = \arcsin\left(\frac{k_y - \frac{e}{c} A_{1,2,3}}{k}\right).$$

Here we define inward and outward solutions as $\Phi_{A,B}(x=0)$ and $\Phi_{A,B}(x = N\Delta x)$ respectively. Thus, the solution for inward waves and the outward wave becomes

$$\Phi_{in} = \begin{pmatrix} \Phi_A(x=0) \\ \Phi_B(x=0) \end{pmatrix} = \begin{pmatrix} 1+r \\ e^{i\theta_0} - re^{-i\theta_0} \end{pmatrix} \begin{pmatrix} \Phi_A(x) \\ \Phi_B(x) \end{pmatrix} \quad (11)$$

and

$$\Phi_{out} = \begin{pmatrix} \Phi_A(x = N\Delta x) \\ \Phi_B(x = N\Delta x) \end{pmatrix} = \begin{pmatrix} t \\ te^{i\theta_e} \end{pmatrix} \begin{pmatrix} \Phi_A(x) \\ \Phi_B(x) \end{pmatrix} \quad (12)$$

respectively, where θ_0 and θ_e is the angle of injected electron for the inward and outward region. Using Φ_{in} and Φ_{out}, we can solve for the transmission coefficient t, as

$$t = \frac{2\cos\theta_0}{(x_{22}e^{-i\theta_0} + x_{11}e^{i\theta_e}) - x_{12}e^{i(\theta_e - \theta_0)} - x_{21}}. \quad (13)$$

For the AP and P alignment of magnetic barriers, we replace X in eq. (9) with the corresponding series of M_j in eq. (8) for each pattern. Thus, the transmission coefficient becomes t_{AP} and t_P with above the substitution.

To determine the conditions for the enhancement of magnetoresistance (MR), we can calculate the difference between the conductance of a magnetic structure on parallel (G_P) and antiparallel (G_{AP}) magnetization configurations. It can be calculated by the equation below.

$$MR = \frac{G_{AP} - G_P}{G_P} \times 100\% \quad (14)$$

The charge conductance $G_{AP,P}$ is given by

$$G_{AP,P} / G_0 = \left\langle T_{AP,P} \right\rangle = \int_{-\pi/2}^{\pi/2} \left| t_{AP,P}(\theta) \right|^2 \cos(\theta) d\theta \quad (15)$$

where $G_0 = 2e^2 E_F L_y / (\pi\hbar)^2$ and L_y is the sample size in the y direction. θ is the angle of incidence in the x-direction and $T_{AP,P}$ is the transmission probabilities that can be calculated using the transfer-matrix method.

3. Result and Discussion

In this section, we study the transport properties of relativistic electron collimation propagating through a graphene structure with multiple periodic MVP barriers. To collimate electron gas (2DEG), graphene must be doped by applying high gate voltage. The collimation angle of the transmitted electron parallelizes the x-axis. It allows us to understand the transport behavior of the relativistic particle. In the case of the magnetic barrier without electrostatic potential, the conductance for different values of the magnetic energy in the antiparallel and parallel alignment of magnetic structures are shown in Fig. 2. For the AP structure with zero spatial average, we found that the lowest position of the transmission probabilities of collimated electron change with the number of periods of the MVP barriers. The result indicates that the Dirac-point position shift toward the positive Fermi energy as a function of the number of MVP barriers. When the Fermi energy shift is plotted by comparing with the number of periodic barriers as shown in Fig. 3. We found that the relationship between the two quantities is linear where the slope changes as the result of the width of the magnetic barrier. Therefore, it can be seen that the characteristic of this quantity can lead to easier control of the Dirac point position by manipulating the number of barriers.

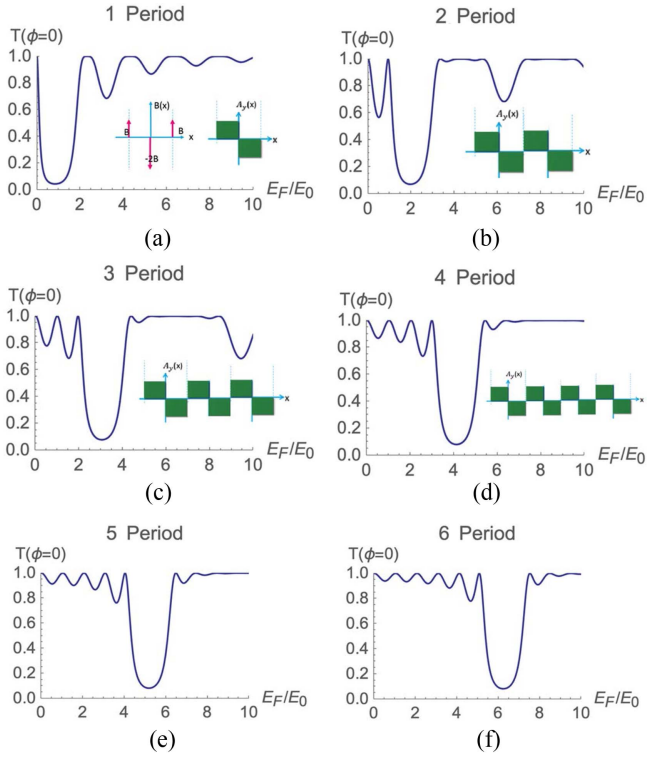

Fig. 2. (Color online) The transmission probability of collimated Dirac electrons vs. the Fermi energy for the antiparallel magnetic structures. The (a)-(f) refer to the system with the MVP barriers from 1 to 6 periods, respectively. The insets show the antiparallel shapes of the magnetic field of delta-function barriers and MVP profiles on the surface of graphene.

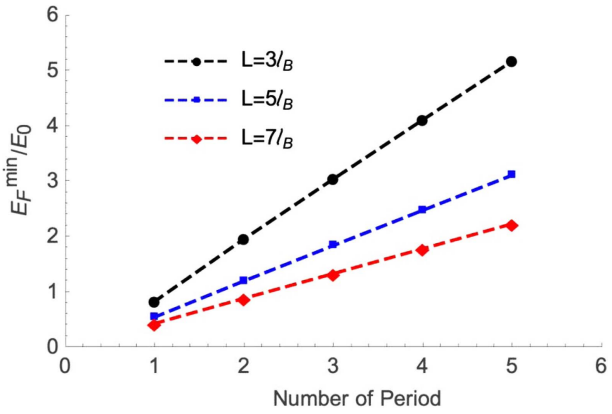

Fig. 3. (Color online) The Fermi energy with the lowest possible transmission versus the period of the potential by adjusting the value of the period width.

For the P structures with low magnetic energy, we appear zero-conductance regions because it is not a zero-on-average periodic magnetic field that leads to the occurrence of gap-opening near the Dirac point as shown in Fig. 4. We found that the lowest position of the

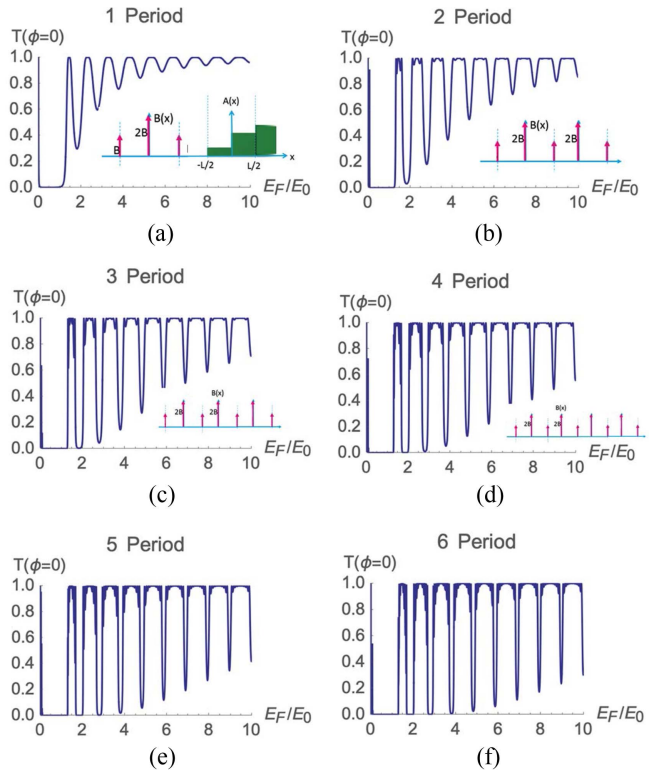

Fig. 4. (Color online) The transmission probability of collimated Dirac electrons plotted relative to the Fermi energy for the parallel structures. (a)-(f) The (a)-(f) refers to the system with the MVP barriers from 1 to 6 periods, respectively. insets show the parallel shapes of the magnetic field of delta-function barriers and MVP profiles on the surface of graphene.

transmission probability does not change with the number of periods of the MVP barriers. This is different from a parallel building which changes as the magnetic structure increases the number of periods. This result indicates that there is an energy gap from the magnetic potential effect where electrons are localized in those structures. Increasing the number of periods of this magnetic structure affects the behavior of resonant transmission where the resonant peak splitting occurs. With an increase in the number of periods, the number of resonant peaks is split up, which results in a band of perfect transmission regions.

In the case of periodic magnetic barriers with electrostatic potential, the conductance for two patterns of electrostatic potential in the AP structure are shown in Fig. 5(a) and 5(b), respectively. Fig. 5(a) shows the effect of the electrostatic potential pattern on the magnetic alignment structure on the $G(E_F)$. For the presence of the electric field effect, U_A ($U_1 = U_2$), the conductance peak at the low E_F decreases approximately linearly with increasing electrostatic potential. The position of the conductance peak is shifted to higher E_F with higher U,

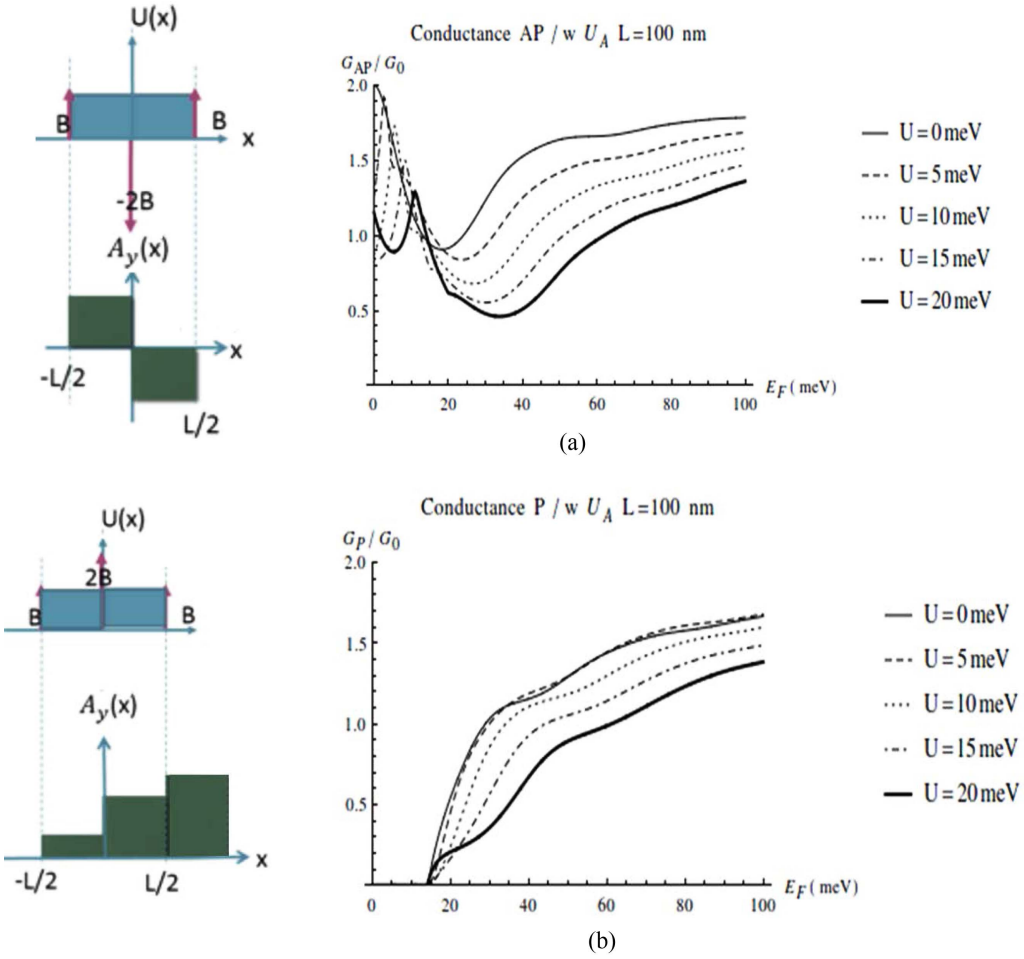

Fig. 5. (Color online) Conductance vs Fermi energy in graphene with gate potential U_A.

but for the asymmetric case of U_B ($U_1 = -U_2$) in Fig. 5(b), the peak height reduced rapidly, and the width increased as gate potential increased. For the case of parallel alignment of the magnetization structure, the curves of their conductivity are not different significantly due to changes in the pattern characteristic of the gate potential as shown in Fig. 6(a) and 6(b). In both cases, the pattern of potentials cannot perturb the band-gap width.

From the result in Fig. 5 and Fig. 6, it appears the 100 % TMR plateaus to be stable in every potential energy when E_F is less than $2E_0$ but for the case of the U_B pattern, the TMR exhibits oscillatory behavior with decaying exponential amplitude when $E_F > 2E_0$ as shown in Fig. 7(b). With the applied U_A pattern on magnetic barrier structure, it shows that TMR has changed from 100 % to 0 % as well as decreases approximately linearly with increasing Fermi energy as shown in Fig. 7(a).

4. Conclusion

The effect of electrostatic potential patterns on electrical properties and magnetoresistance was studied in graphene junctions with two types of multiple periodic barriers. In this system, the direction of magnetization can be changed from parallel to antiparallel magnetic configuration. Typically, the electrons in graphene are unique in carrying the potential barrier charge without reflection at zero degrees relative to the direction of motion resulting from the behavior of the relativistic quantum effect which is called the phenomenon of Klein tunneling. This phenomenon makes it impossible to completely cut off the current flowing in graphene-based circuits. So, it is difficult to achieve 100 % complete magnetoresistance using only normal gate potential in proximity-induced ferromagnetic graphene. To solve this problem, Klein's

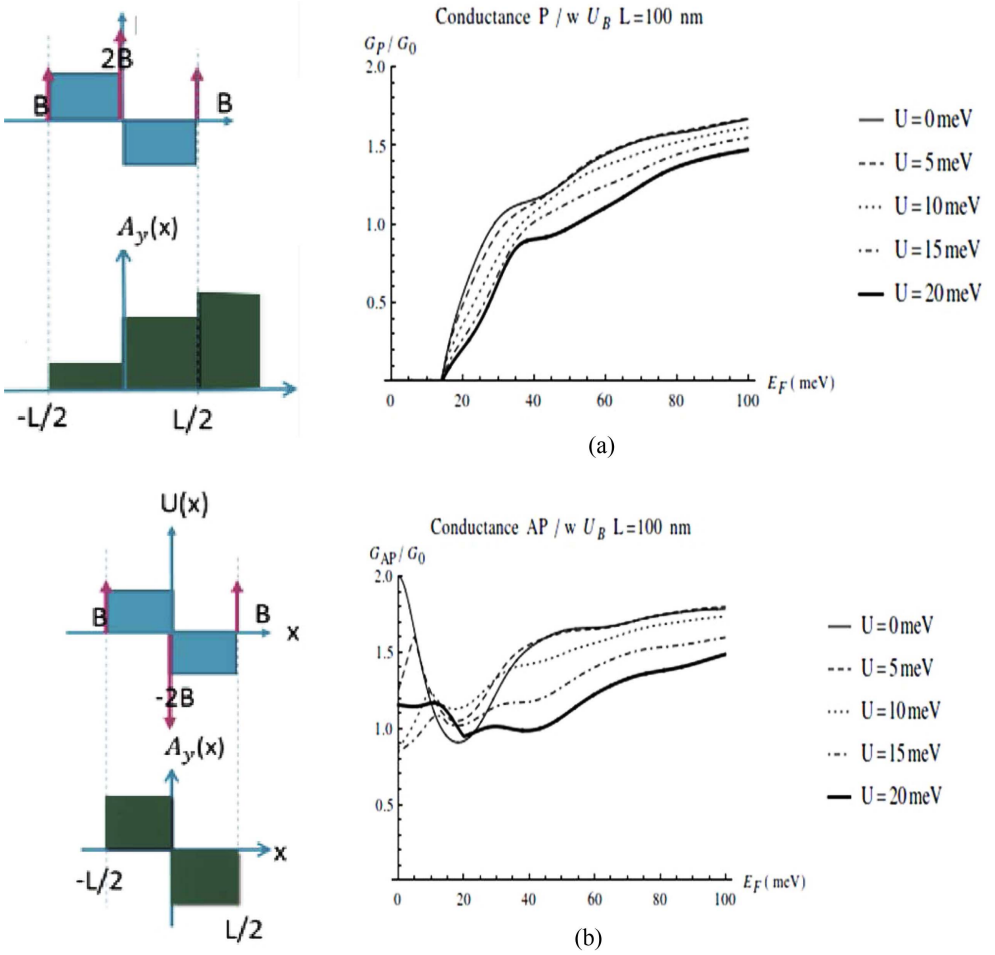

Fig. 6. (Color online) Conductance vs Fermi energy in graphene with gate potential U_B.

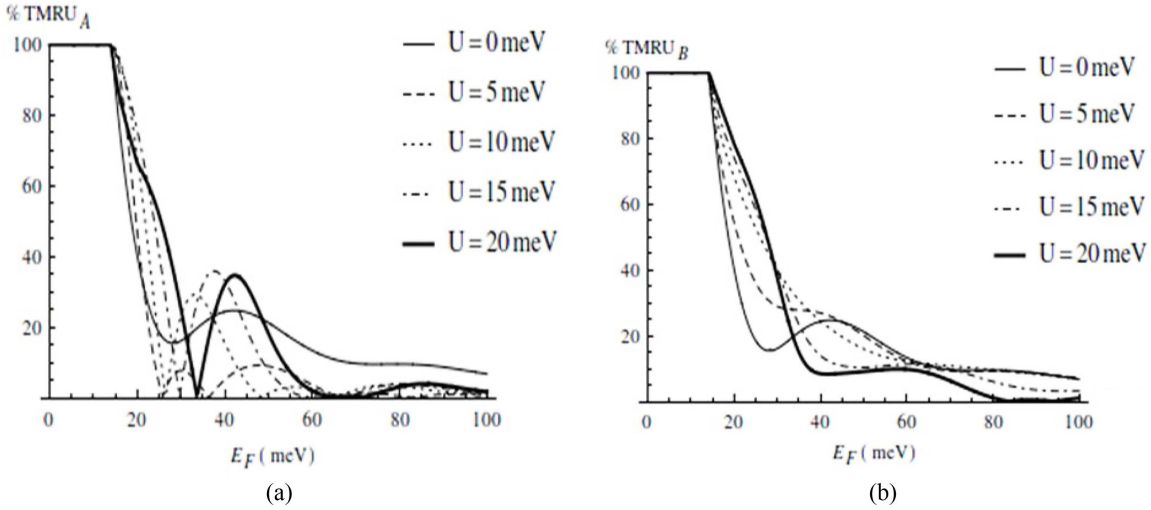

Fig. 7. Tunneling magnetoresistance vs Fermi energy with controllable gate potential in the case of (a) U_A and (b) U_B.

quantum tunneling could be eliminated by using a parallel magnetic barrier to generate an MVP on the graphene. For the transition from parallel to the antiparallel configuration of the magnetic structure, the Klein tunneling is resumed. This will cause the transmission of electrons to be very high. Thus, the transmission probability and

conductivity between the two magnetic field structures are significantly different. By modifying this magnetic structure, we can create new techniques for controlling electrons in graphene to design and build a complete magnetoresistance device. It can also be further developed into a transistor design.

Acknowledgment

The first author would like to thank you Bansomdejchaopraya Rajabhat University (BSRU) for its financial support.

References

[1] K.S. Novoselov, D. Jiang, F. Schedin, T. Booth, V. Khotkevich, S. Morozov and A.K. Geim, Proc. Natl. Acad. Sci. U.S.A. **102**, 10451 (2005).
[2] M. I. Katsnelson, K. S. Novoselov, and A. K. Geim, Nature Physics. **2**, 620 (2006).
[3] K. S. Novoselov, A. K. Geim, S. V. Morozov, D. Jiang, M. I. Katsnelson, I. V. Grigorieva, S. V. Dubonos, and A. A. Firsov, Nature **438**, 197 (2005).
[4] P. M. Krstajic and P. Vasilopoulos, J. Phys. Condens. Matter **23**, 135302 (2011).
[5] N. M. R. Peres, J. Phys: Condens. Matter **21**, 095501 (2009).
[6] A. H. Castro Neto, F. Guinea, N. M. R. Peres, K. S. Novoselov, and A. K. Geim, Rev. Mod. Phys. **81**, 109 (2009).
[7] H. Haugen, D. Huertas-Hernando, and A. Brataas, Phys. Rev. B **77**, 115406 (2008).
[8] C. Saipaopan, W. Choopan, and W. Liewrian, J. Supercond. Nov. Magn. **34**, 2573 (2021).
[9] H. X. Yang, A. Hallal, D. Terrade, X. Waintal, S. Roche, and M. Chshiev, Phys. Rev. Lett. **110**, 046603 (2013).
[10] A. Hallal, F. Ibrahim, H. Yang, S. Roche, and M. Chshiev, 2D Mater. **4**, 025074 (2017).
[11] Z. Wang, C. Tang, R. Sachs, Y. Barlas, and J. Shi, Phys. Rev. Lett. **114**, 016603 (2015).
[12] S. Dushenko, H. Ago, K. Kawahara, T. Tsuda, S. Kuwabata, T. Takenobu, T. Shinjo, Y. Ando, and M.Shiraishi, Phys. Rev. Lett. **116**, 166102 (2016).
[13] J. C. Leutenantsmeyer, A. A. Kaverzin, M. Wojtaszek, and B. J. van Wees, 2D Mater. **4**, 014001 (2017).
[14] P. Wei, S. Lee, F. Lemaitre, L. Pinel, D. Cutaia, W. Cha, F. Katmis, D. Heiman, J. Hone, J. S. Moodera, and C. T. Chen, Nat. Mater. **15**, 711 (2016).
[15] A. G. Swartz, P. M. Odenthal, Y. Hao, R. S. Ruoff, and R. K. Kawakami, ACS Nano. **6**, 10063 (2012).
[16] E. I. Rashba, Phys. Rev. B. **62**, R16267(R) (2000).
[17] Y. Ohno, D. K. Young, B. Beschoten, F. Matsukura, H. Ohno, and D. D. Awschalom, Nature. **402**, (1999).
[18] A. Fert and H. Jaffrès, Phys. Rev. B. **64**, 184420 (2001).
[19] Y. W. Son, M. L. Cohen, and S. G. Louie, Nature **444**, 347 (2006).
[20] Y.G. Semenov, K. W. Kim, and J. M. Zavada, Appl. Phys. Lett. **91**, 153105 (2007).
[21] T. Yokoyama, Phys. Rev. B **77**, 073413 (2008).
[22] C. Saipaopan, W. Choopan, and W. Liewrian, Physica E. **115**, 113625 (2020).
[23] F. Zhai, and K. Chang, Phys. Rev. B. **77**, 113409, (2008).
[24] W. Liewrian, R. Hoonsawat, and I. M. Tang, Physica E. **44**, 327 (2011).
[25] Y. Song and G. Dai, Appl. Phys. Lett. **106**, 223104 (2015).
[26] Y. Song, J. Phy. D: Appl. Phys. **51**, 025002 (2018).
[27] Y. Song, Y. Liu, X. Feng, F. Yan, and W. Zhang, Phys. Chem. Chem. Phys. **20**, 10.1039/c7cp06871a (2017).
[28] L. Dell'Anna1 and A. De Martino, Phys. Rev. B **80**, 155416 (2009).
[29] S. Ghosh and M. Sharma. J. Phys.: Condens. Matter. **21**, 292204, (2009).
[30] N. Agrawal (Garg), S. Ghosh, and M. Sharma, Int. J. Mod. Phys. B **27**, 1341003 (2013).